Proceedings of the IMAC-XXVII
February 9-12, 2009 Orlando, Florida USA

Dynamic Error Correction of Force Sensor

Yusaku Fujii
Professor, Department of Electronic Engineering, Faculty of Engineering
1-5-1 Tenjin-cho, Kiryu, Gunma 376-8515, Japan

Abstract

The author has proposed a method, the Levitation Mass Method (LMM). In the LMM, the inertial force of a mass levitated using a pneumatic linear bearing is used as the reference force applied to the objects under test, such as force sensors, materials or structures. The inertial force of the levitated mass is measured using an optical interferometer. The author has modified it as calibration methods for the three typical types of the dynamic forces, that are the dynamic calibration method under impact load, the dynamic calibration method under oscillation load and the dynamic calibration method under step load. Recently, a method for evaluating and correcting the effect of the inertial mass on dynamic force measurements has been proposed based on the LMM. In this paper, the recent achievement and the future prospects on the methods and the instruments for correcting the effect of the inertial mass on dynamic force measurements based on the LMM are discussed.

Keywords: Inertial force, Inertial mass, Dynamic force, Pneumatic bearing, Air bearing, Optical interferometer

1. Introduction

Force is one of the basic physical quantities and is defined as the product of mass and acceleration. The need for measuring dynamic forces have increased in various industrial and research applications such as process monitoring, material testing, motion control and crash testing. However, force sensors are typically calibrated by standard static methods using static weights under static conditions. At present, there are no standard methods of evaluating the dynamic characteristics of force sensors. This results in two major problems in measuring varying force. One is that it is difficult to evaluate the uncertainty of the measured varying force. The other is that it is difficult to evaluate the uncertainty of the moment at which the varying force is measured.

The author has proposed and developed a method for precision mass and force measurement, the levitation mass method (LMM), in which the inertial force of a mass levitated using a pneumatic linear bearing is used as the reference force applied to the objects under test, such as force sensors, materials or structures. The inertial force of the mass is measured using an optical interferometer. In the LMM, only the motion-induced Doppler shift frequency is measured during the measurement. All the other quantities, such as velocity, position, acceleration and force, are numerically calculated from the frequency. This results in the good synchronization between the obtained quantities. In addition, force is directly calculated according to its definition, that is, the product of mass and acceleration.

The author has modified it as calibration methods for all the three categories of the dynamic force calibration [1,2,3], that are the dynamic calibration method under impact load [1], the dynamic calibration method under oscillation load [2] and the dynamic calibration method under step load [3].

The author has applied the LMM for material testing without using force sensors, such as methods for evaluating material viscoelasticity under an oscillating load [4] and under an impact load [5,6], a method for evaluating material friction [7,8], a method for evaluating biomechanics [9-10], a method for measuring body-mass of astronauts for use under microgravity conditions [11-12], a method for evaluating dynamic response of impact hammers [13] and a method for generating and measuring static and dynamic micro-Newton level forces [14-17].

The author has also applied the LMM as a method for investigating the frictional characteristics of pneumatic linear bearings [18,19] and the linear ball bearing [20]. To improve the efficiency of the LMM, a pendulum mechanism [21] for use as a substitute of a pneumatic linear bearing and a frequency measurement technique [22,23] using a digitizer instead of an electronic frequency counter, have been developed. Recently, a method for correcting the effect of the inertial mass on dynamic force measurements has been proposed based on the LMM [24,25].

As for the dynamic calibration method for force sensors, a method for calibrating sensors against oscillation force has also been proposed by Kumme [26,27]. In this method, both the mass and the sensor are shaken at a single frequency using a shaker, and the inertial force of the mass is applied to the sensor. Park et al. use this method for dynamic investigation of multi-component force-moment sensors [28,29]. However, it has not yet been established how to apply the results of such dynamic calibration methods, including those proposed by the author, to the actual wave profile of the varying force.

In this paper, the recent achievement and the future prospects on the methods and the instruments for correcting the effect of the inertial mass on dynamic force measurements based on the LMM are discussed.

2. Experimental setup

Figure 1 shows a schematic diagram of the experimental setup for measuring the effect of the inertial force of a part of the force sensor itself. Figure 2 shows the photograph around the test section. A conventional S-shaped strain-gauge-type force sensor is attached to the base. A pneumatic linear bearing is used to realize a horizontal linear motion with sufficiently small friction acting on a mass, i.e., the moving part of the bearing.

Two optical interferometers, Interferometer-1 and Interferometer-2, are built to measure the velocity of the mass and the sensing point of the force sensor, respectively. The mass of the moving part, including a cube corner prism, $\boldsymbol{M}_1$, is approximately 2.65 kg. The mass of the metal plate attached to the force sensor including the cube corner prism, M_2, is approximately 0.082 kg.

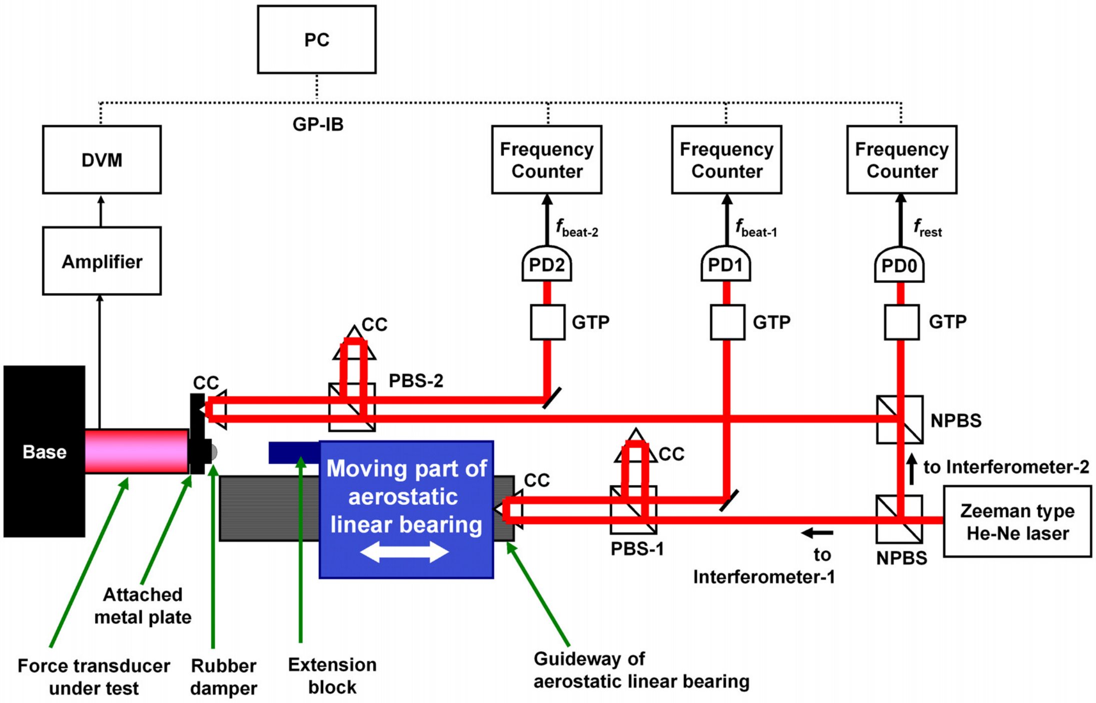

Figure 1. Experimental setup. Code: CC= cube corner prism, PBS= polarizing beam splitter, NPBS= non- polarizing beam splitter, GTP= Glan-Thompson prism, PD= photo diode, LD= laser diode, ADC=analog-to-digital converter, DAC= digital-to-analog converter, PC= computer.

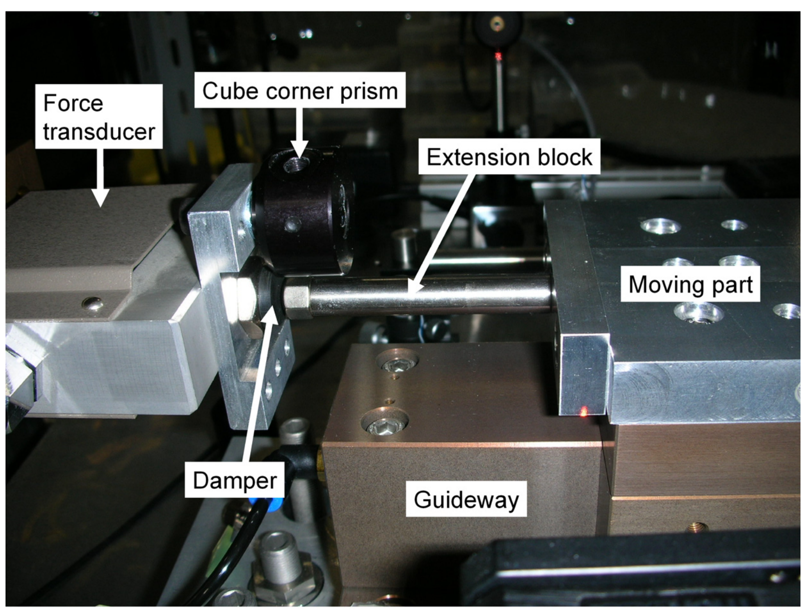

Figure 2. Photograph around test section.

A Zeeman-type two-frequency He-Ne laser is used as the light source of the optical interferometers. The interferometers have three photo-detectors: PD0, PD1 and PD2. The frequency difference between the two orthogonal polarization states emitted from the laser, $\boldsymbol{f}_{\mathbf{rest}}$, is monitored using a Glan-Thompson prism (GTP) and the first photo-detector, PD0.

The total force acting on the moving part of the aerostatic linear bearing, $\boldsymbol{F}_{\mathbf{mass}}$, is calculated as the product of its mass, $\boldsymbol{M}_1$, and its acceleration, $\boldsymbol{a}$, as follows:

$$\boldsymbol{F}_{\mathbf{mass}} = \boldsymbol{M}_1 \boldsymbol{a}.$$

In the measurement, the total force acting on the mass, $\boldsymbol{F}_{\mathbf{mass}}$, is considered to be the same as the force acting on the mass from the force sensor being tested, since the frictional force acting on the mass is negligible [8]. The acceleration is calculated from the velocity of the levitated mass. The velocity of the mass, i.e. of the moving part of the aerostatic linear bearing, $\boldsymbol{v}_1$, is measured as the Doppler shift frequency, $\boldsymbol{f}_{\mathbf{Doppler-1}}$, which can be expressed as follows:

$$\boldsymbol{v}_1 = \lambda_{\mathbf{air}} (\boldsymbol{f}_{\mathbf{Doppler-1}})/2 ,$$

$$\boldsymbol{f}_{\mathbf{Doppler-1}} = - (\boldsymbol{f}_{\mathbf{beat-1}} - \boldsymbol{f}_{\mathbf{rest}}),$$

where $\lambda_{\mathbf{air}}$ is the wavelength of the signal beam under the experimental conditions, and $\boldsymbol{f}_{\mathbf{beat-1}}$ is the beat frequency, which is the frequency difference between the signal beam and the reference beam and appears as the beat frequency at PD1. In this case, the linear polarization transmitted through the polarizing beam splitter PBS-1, whose frequency is larger than that of the other linear polarization, is used as the signal beam. The direction of the coordinate system for the velocity, acceleration and force acting on the moving part is toward the right in Figure1. The position of the mass $\boldsymbol{x}_1$, the acceleration of the mass $\boldsymbol{a}_1$ and the force acting on the mass, $\boldsymbol{F}_{\mathbf{mass}}$, are numerically calculated from the velocity.

On the other hand, the velocity of the sensing point of the force sensor, $\boldsymbol{v}_2$, which is attached to the right side of the sensor being tested, is measured as the Doppler shift frequency, $\boldsymbol{f}_{\mathbf{Doppler-2}}$, which can be expressed as follows:

$$\boldsymbol{v}_2 = \lambda_{\mathbf{air}} (\boldsymbol{f}_{\mathbf{Doppler-2}})/2 ,$$

$$\boldsymbol{f}_{\mathbf{Doppler-2}} = - (\boldsymbol{f}_{\mathbf{beat-2}} - \boldsymbol{f}_{\mathbf{rest}}),$$

The beat frequency $\boldsymbol{f}_{\mathbf{beat-2}}$ is measured using PD2. The position $\boldsymbol{x}_2$ and the acceleration $\boldsymbol{a}_2 = \boldsymbol{a}_{\mathbf{sensor}}$ of the actuator are numerically calculated from the velocity $\boldsymbol{v}_2$.

The frequency $\boldsymbol{f}_{\mathbf{beat-1}}$ appearing at PD1 is measured using an electric frequency counter (model: R5363; manufactured by Advantest Corp., Japan). It continuously measures and records the beat frequency, $\boldsymbol{f}_{\mathbf{beat-1}}$, 1000 times at a sampling interval of $T=400/\boldsymbol{f}_{\mathbf{beat-1}}$, and stores the values in its memory. This counter continuously measures the interval time every 400 periods without dead time. The sampling period of the counter is approximately 0.15 ms at a frequency of 2.7 MHz. Two other counters of the same model measure the frequencies $\boldsymbol{f}_{\mathbf{rest}}$ and $\boldsymbol{f}_{\mathbf{beat-2}}$ appearing at PD0 and PD2, respectively. The counters measure the frequencies without dead time and the sampling interval, $\boldsymbol{T}$, can be exactly calculated using the measured frequency, $\boldsymbol{f}$, and the expression $\boldsymbol{T}=400/\boldsymbol{f}$.

The aerostatic linear bearing, Air-Slide TAAG10A-02 (NTN Co., Ltd., Japan), is attached to an adjustable tilting stage. The maximum weight of the moving part is approximately 30 kg, the thickness of the air film is approximately 8 μm, the stiffness of the air film is more than 70 N/μm, and the straightness of the guideway is better than 0.3 μm /100 mm. The frictional characteristics were determined in detail by means of the developed method [18,19].

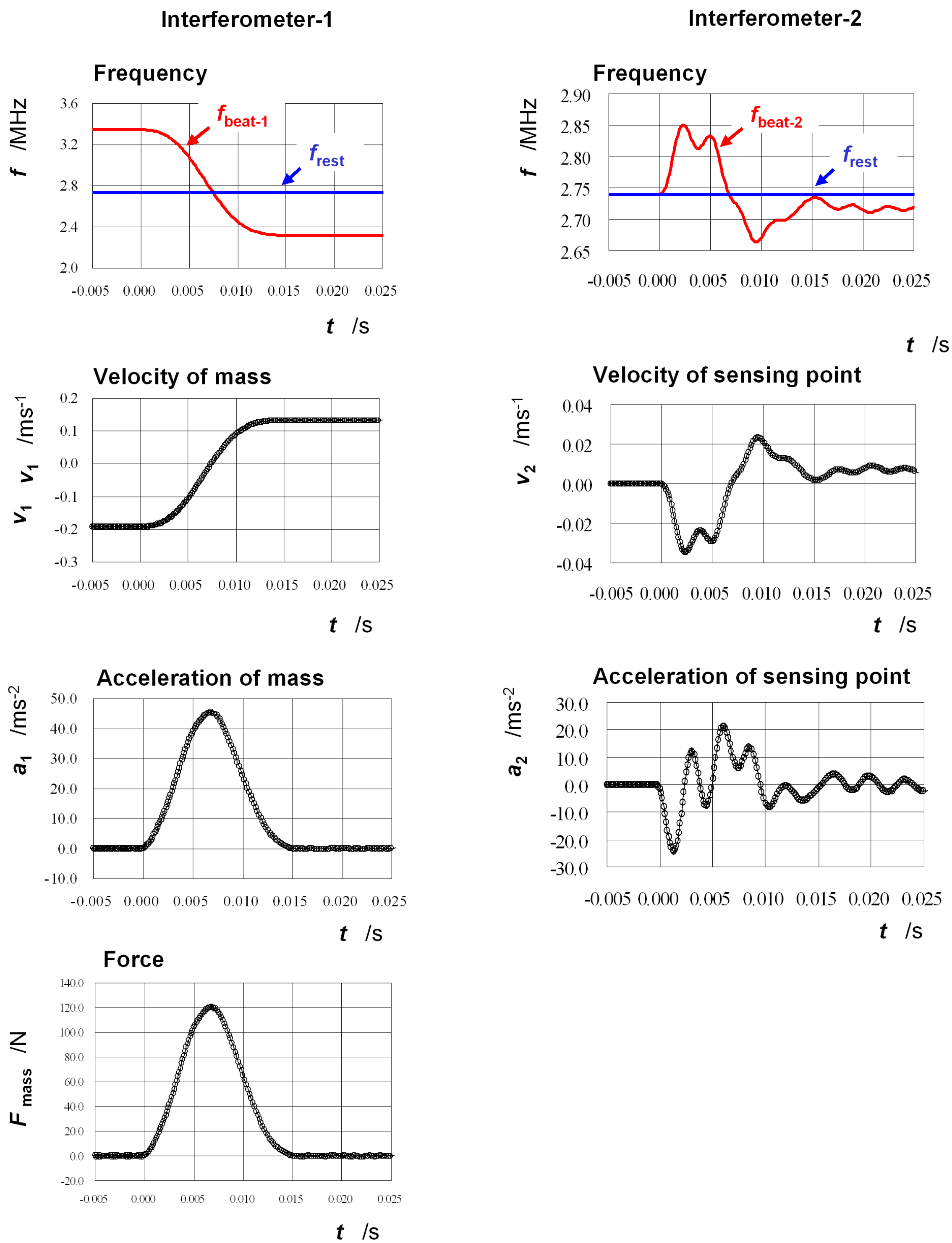

Figure 3. Data processing procedure: calculation of the velocity, position, acceleration and force from the measured frequency.

The output signal of the force sensor is measured using a digital voltmeter (model: VP5481L; manufactured by Panasonic Corp., Japan) at a sampling interval of 0.2 ms.

The measurements using the three electric counters (R5363) and the digital voltmeter (VP5481L) are triggered by means of a sharp trigger signal generated using a digital-to-analog converter (DAC). This signal is initiated by means of a light switch, a combination of a laser diode and a photodiode. In the experiment, one collision measurement was conducted and the electric and mechanical responses of the sensors were measured.

In the experiment, 1 set of collision measurement is conducted.

3. Results

Figure 3 shows the data processing procedure in the collision experiment. During the collision experiment, the frequencies $\boldsymbol{f}_{\mathbf{rest}}$, $\boldsymbol{f}_{\mathbf{beat-1}}$ and $\boldsymbol{f}_{\mathbf{beat-2}}$ were measured using the photodiodes PD0, PD1 and PD2, respectively. The velocity $\boldsymbol{v}_{\mathbf{1}}$, acceleration $\boldsymbol{a}_{\mathbf{1}}$ and inertial force $\boldsymbol{F}_{\mathbf{mass}}$ of the moving part of the bearing were calculated from $\boldsymbol{f}_{\mathbf{rest}}$ and $\boldsymbol{f}_{\mathbf{beat-1}}$ measured using Interferometer-1. The velocity $\boldsymbol{v}_{\mathbf{2}}$ and acceleration $\boldsymbol{a}_{\mathbf{2}}$ of the sensing point of the sensor were calculated from $\boldsymbol{f}_{\mathbf{rest}}$ and $\boldsymbol{f}_{\mathbf{beat-2}}$ measured using Interferometer-2.

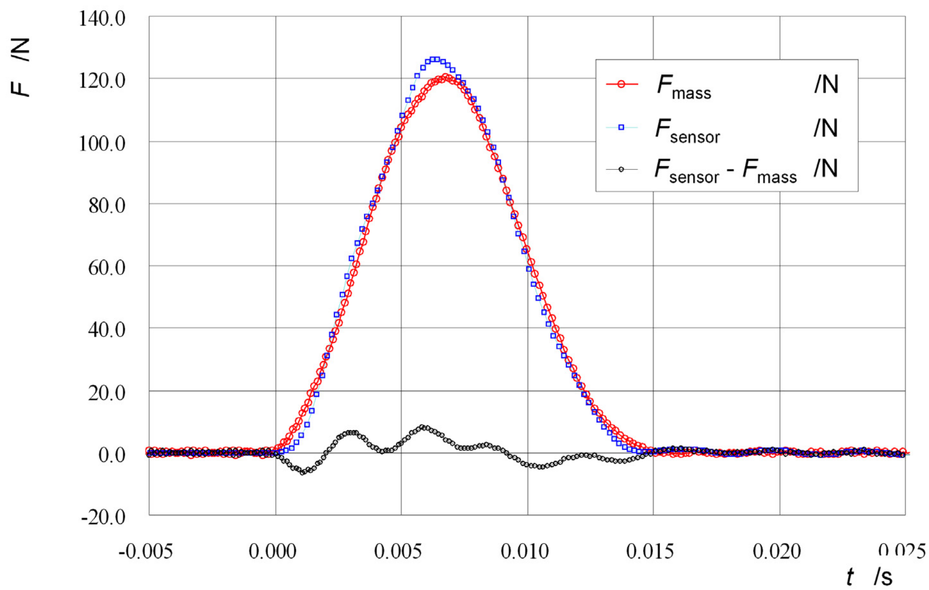

Figure 4. The force acting on the mass, F_{mass} (=$\boldsymbol{M}_{mass}$ a_{mass}), the force calculated from the output signal of the force transducer and its static calibration results $\boldsymbol{F}_{sensor}$, and their difference $\boldsymbol{F}_{sensor}$ - $\boldsymbol{F}_{mass}$.

Figure 4 shows the force acting on the mass, $\boldsymbol{F}_{\mathbf{mass}}$ (=$\boldsymbol{M}_{\mathbf{mass}}$ $\boldsymbol{a}_{\mathbf{1}}$ =$\boldsymbol{M}_{\mathbf{mass}}$ $\boldsymbol{a}_{\mathbf{mass}}$), the force calculated from the output signal of the force sensor and its static calibration results $\boldsymbol{F}_{\mathbf{sensor}}$, and their difference $\boldsymbol{F}_{\mathbf{sensor}}$ - $\boldsymbol{F}_{\mathbf{mass}}$. The difference between $\boldsymbol{F}_{\mathbf{sensor}}$ and $\boldsymbol{F}_{\mathbf{mass}}$ derived mainly form the difference between the static characteristics and the dynamic characteristics of the sensor.

Figure 5 shows the relationship between the acceleration of the sensing point $\boldsymbol{a}_{\mathbf{2}}$ = $\boldsymbol{a}_{\mathbf{sensor}}$ and the difference between the values measured by the sensor and those measured by the proposed method, $\boldsymbol{F}_{\mathbf{sensor}}$ - $\boldsymbol{F}_{\mathbf{mass}}$. The regression line, $\boldsymbol{F}$ = 0.31 $\boldsymbol{a}_{\mathbf{sensor}}$, is also shown in the figure. A good correlation was estimated from the figure. If the sensor is considered as a mechanical structure consisting of an inertial mass and a spring element, and if the output signal can be considered to represent the deformation of the spring, the inclination of the line, 0.31, can be considered as the estimated effective inertial mass of the sensor, $\boldsymbol{M}_{\mathbf{estimated}}$. $\boldsymbol{F} = \boldsymbol{M}_{\mathbf{estimated}}\ \boldsymbol{a}_{\mathbf{sensor}}$. The value $\boldsymbol{M}_{\mathbf{estimated}} - \boldsymbol{M}_{\mathbf{2}}$ was calculated to be 0.23 kg, which corresponds to 60 % of the total mass of the sensor itself. Since the sensor is S-shaped and its deformation is designed to concentrate around the center of the sensor, the result which estimates the effective inertial mass at about half of the mass of the sensor is reasonable.

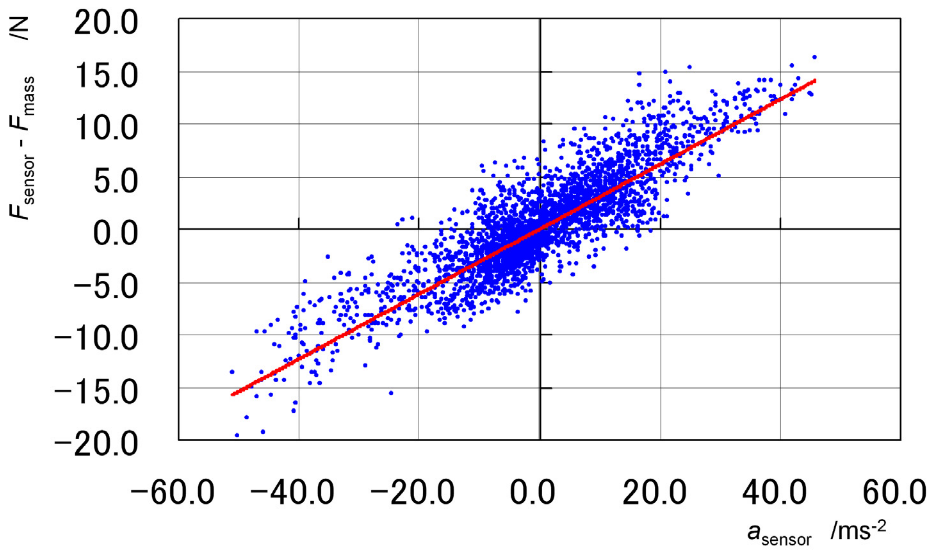

Figure 5. Relationship between the acceleration measured using the accelerometer $\boldsymbol{a}_{\mathrm{sensor}}$ and the difference between the values measured using the transducer and those measured by the proposed method, $\boldsymbol{F}_{\mathrm{sensor}} - \boldsymbol{F}_{\mathrm{mass}}$. The regression line, $\boldsymbol{F}_{\mathrm{reg}}$=0.31 $\boldsymbol{a}_{\mathrm{sensor}}$, is also shown.

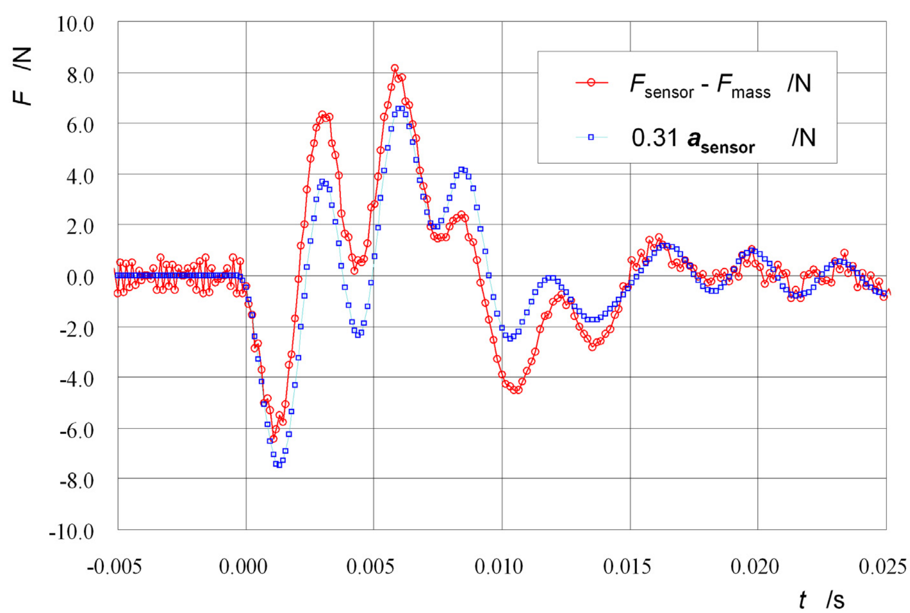

Figure 6. Difference between the values measured by the transducer and those measured by the proposed method, and the estimated inertial force of the sensor element.

Figure 6 shows the difference between the values measured by the sensor and those measured by the proposed method, $\boldsymbol{F}_{\mathbf{sensor}} - \boldsymbol{F}_{\mathbf{mass}}$, and the estimated inertial force of the sensor element, $\boldsymbol{F} = \boldsymbol{M}_{\mathbf{estimated}}\ \boldsymbol{a}_{\mathbf{sensor}} = 0.31\ \boldsymbol{a}_{\mathbf{sensor}}$.

4. Discussions

The possible causes for the difference between the static and dynamic characteristics of the output electric signal of strain-gauge-type force sensors are as follows:

(1) Inertial mass: the effect of the inertial force of the inertial mass of a part of the sensor.
(2) Strain gauge: the difference between the static and dynamic characteristics of the strain gauge.
(3) Elastic body: the difference between the static and dynamic characteristics of the elastic body.
(4) Signal processor: the difference between the static and dynamic characteristics of the electric signal processing system.

In the experiment using the S-shaped strain-gauge-type force sensor, the effect of the inertial mass was dominant. As shown in Figure 6, the simple spring-mass model explained the difference between the static and dynamic characteristics of the output electric signal well. However, some discrepancy is still observed. This indicates that there is still some room for improvement. If a more sophisticated mechanical model, such as a finite element model, is adopted and the distribution of the acceleration and the inertial force inside the sensor are considered, the accuracy of the correction might be improved.

If the accelerometer is attached to the S-shaped strain-gauge-type force sensor used in the experiment, then the correction for the dynamic measurement error caused by the effect of inertial force acting on a part of the sensor structure itself can be done using the output signal of the accelerometer attached.

Since the output signal of the force sensor is thought to be almost proportional to the deformation of the sensor structure, and then the acceleration of the sensing point of the sensor is proportional to differential coefficient of second order of the output signal of the force sensor. Therefore, the correction for effect of inertial force acting on a part of the sensor structure itself could be done using only the output signal of the force sensor itself.

5. Conclusions

The present status and the future prospects on the dynamic error correction of force sensor based on the Levitation Mass Method (LMM) are reviewed. The authors think that the LMM is the key to develop and establish a method for evaluating and correcting the dynamic measurement error of force sensors.

Acknowledgement

This work was supported by the Grant-in-Aid for Scientific Research (B) 19360185 (KAKENHI 19360185) and the research-aid fund of the Asahi Glass Foundation.

References

[1] Y. Fujii, “Measurement of steep impulse response of a force transducer”, Meas. Sci. Technol. 14(1), 65-69 (2003).

[2] Y. Fujii, “A method for calibrating force transducers against oscillation force”, Meas. Sci. Technol. 14(8), 1259-1264 (2003).

[3] Y. Fujii, “Proposal for a step response evaluation method for force transducers”, Meas. Sci. Technol. 14(10), 1741-1746 (2003).

[4] Y. Fujii and T. Yamaguchi, “Method for evaluating material viscoelasticity”, Rev. Sci. Instrum. 75(1), 119-123 (2004).

[5] Y. Fujii and T. Yamaguchi, ”Proposal for material viscoelasticity evaluation method under impact load ”, Journal of Materials Science 40(18), 4785 – 4790 (2005).

[6] Y. Fujii and D.W. Shu, “Impact force measurement of an actuator arm of a hard disk drive”, Int. J. Impact Eng. 35(2), 980-108 (2008).

[7] Y. Fujii and T. Yamaguchi, “Optical method for evaluating material friction”, Meas. Sci. Technol. 15(10), 1971-1976 (2004).

[8] Y. Fujii, "Method for Measuring Transient Friction Coefficients for Rubber Wiper Blades on Glass Surface", Tribology International 41(1), 17-23 (2008).

[9] Y. Fujii, T. Yamaguchi and J. Valera, “Impact response measurement of a human arm”, Experimental Techniques 30(3), 64-68 (2006).

[10] Y. Fujii and T. Yamaguchi, "Method of evaluating the force controllability of human finger", IEEE Trans. Instrum. Meas. 55(4), 1235-1241 (2006).

[11] Y. Fujii and K. Shimada, "Instrument for measuring the mass of an astronaut", Meas. Sci. Technol. 17(10), 2705-2710 (2006).

[12] Y. Fujii and K. Shimada, "The space scale: An Instrument for astronaut mass measurement", Trans. Jpn. Soc. Aeronaut. Space Sci. 50(170), 251-257 (2008).

[13] Y. Fujii, “Optical method for accurate force measurement: dynamic response evaluation of an impact hammer”, Optical Engineering 45(2), 023002-1-7 (2006).

[14] Y. Fujii, “Method for generating and measuring the micro-Newton level forces”, Mech. Syst. Signal Pr. 20(6), 1362-1371 (2006).

[15] Y. Fujii, “Microforce materials tester”, Rev. Sci. Instrum. 76(6), 065111-1-7 (2005).

[16] Y. Fujii, "Microforce materials tester based on the levitation mass method", Meas. Sci. Technol. 18(6), 1678-1682 (2007).

[17] Y. Fujii, "Method of generating and measuring static small force using down-slope component of gravity", Rev. Sci. Instrum. 78(6), 066104-1-3 (2007).

[18] Y. Fujii, “Measurement of force acting on a moving part of a pneumatic linear bearing”, Rev. Sci. Instrum. 74(6), 3137-3141 (2003).

[19] Y. Fujii, “Frictional characteristics of an aerostatic linear bearing”, Tribology International 39(9), 888-896 (2006).

[20] Y. Fujii, “An optical method for evaluating frictional characteristics of linear bearings”, Optics and Lasers in Engineering 42(5), 493-501 (2004).

[21] Y. Fujii, “Pendulum for precision force measurement”, Rev. Sci. Instrum. 77(3), 035111-1-5 (2006).

[22] Y. Fujii and J. Valera, "Impact force measurement using an inertial mass and a digitizer", Meas. Sci. Technol. 17(4), 863-868 (2006).

[23] Y. Fujii, "Impact response measurement of an accelerometer", Mech. Syst. Signal Pr. 21(5), 2072-2079 (2007).

[24] Y. Fujii, "Measurement of the electrical and mechanical responses of a force transducer against impact forces", Rev. Sci. Instrum. 77(8), 085108-1-5 (2006).

[25] Y. Fujii, “Method for correcting the effect of the inertial mass on dynamic force measurements”, Meas. Sci. Technol. 18(5), N13-N20 (2007).

[26] R. Kumme and M Dixon, “The results of comparisons between two different dynamic force measurement systems”, Measurement 10(3), 140-144 (1992).

[27] R. Kumme, “Investigation of the comparison method for the dynamic calibration of force transducers”, Measurement 23(4), 239-245 (1998).

[28] Y-K. Park, R. Kumme and D-I. Kang, “Dynamic investigation of a three-component force-moment sensor”, Meas. Sci. Technol. 13(5), 654-659 (2002).

[29] Y-K. Park, R. Kumme and D-I. Kang, “Dynamic investigation of a binocular six-component force-moment sensor”, Meas. Sci. Technol. 13(8), 1311-1318 (2002).